

Radio detection of SNR G310.7–5.4 with gamma-ray counterpart

Christopher Burger-Scheidlin,^{a,b,c,*} Brianna D. Ball,^d Sanja Lazarević,^{b,e,f} Roland Kothes,^g Robert Brose,^h Jonathan Mackey,^{a,c} Miroslav D. Filipović,^b Zachary J. Smeaton,² Andrew M. Hopkins,ⁱ Dennis Leahy,^j Jennifer L. West^g and Tayyaba Zafar^k

^a*Astronomy & Astrophysics Section, School of Cosmic Physics, Dublin Institute for Advanced Studies, DIAS Dunsink Observatory, Dublin D15 XR2R, Ireland*

^b*Western Sydney University, Locked Bag 1797, Penrith South DC, NSW 2751, Australia*

^c*School of Physics, University College Dublin, Belfield, Dublin D04 V1W8, Ireland*

^d*Department of Physics, University of Alberta, 4-181 CCIS, Edmonton, Alberta T6G 2E1, Canada*

^e*ATNF, CSIRO, Space and Astronomy, PO Box 76, Epping, NSW 1710, Australia*

^f*Astronomical Observatory, Volgina 7, 11060 Belgrade, Serbia*

^g*Dominion Radio Astrophysical Observatory, Herzberg Astronomy & Astrophysics, National Research Council Canada, P.O. Box 248, Penticton, BC V2A 6J9, Canada*

^h*Institute of Physics and Astronomy, University of Potsdam, 14476 Potsdam-Golm, Germany*

ⁱ*School of Mathematical and Physical Sciences, 12 Wally's Walk, Macquarie University, NSW, 2109, Australia*

^j*Department of Physics and Astronomy, University of Calgary, Calgary, Alberta, Canada*

^k*Banting and KIPAC Fellowships: Kavli Institute for Particle Astrophysics & Cosmology (KIPAC), Stanford University, Stanford, CA 94305, USA*

E-mail: cburger@cp.dias.ie

Supernova remnants (SNRs) are known to accelerate particles up to relativistic energies. We have recently discovered a new SNR, G310.7–5.4 at high Galactic latitude using the ASKAP's EMU and POSSUM surveys at 943.5 MHz [1]. The faint, extended object has an apparent size of $30.6' \times 30.6'$ and shows the typical SNR bilateral shell structure. Strong linear polarisation is detected from the bilateral shell regions. It is also one of the faintest known radio SNRs. Furthermore, a spatially coincident gamma-ray source is detected, indicating that the SNR could be accelerating particles to high energies. SNRs at high Galactic latitudes, such as the one presented here, have received attention in recent years as more of them are detected off the Galactic plane. Discovering these objects together with their gamma-ray counterparts can put a new perspective on such sources as these SNRs are expanding in rather unperturbed, low-density environments, with diminished risk of source confusion. This allows to study cosmic ray (CR) acceleration and constrain CR models.

39th International Cosmic Ray Conference (ICRC2025)
15–24 July 2025
Geneva, Switzerland



*Speaker

1. Introduction

Supernova remnants (SNRs) are important when studying the interstellar medium (ISM) and its enrichment, the evolution of our Galaxy, and the origins of Cosmic Rays (CRs). With currently around 310 confirmed SNRs [2], most of these have first been detected by radio surveys. Only about 10 % are detected at high energies (HE) in γ -rays [3], and fewer at very high energies (VHE; e.g. [4]).

The *Evolutionary Map of the Universe* (EMU; [5]) survey from the *Australian Square Kilometre Array Pathfinder* (ASKAP; [6]) aims to map the entire southern sky at the central radio frequency of 943.5 MHz with high angular resolution. More and more extended faint Galactic objects such as the SNR presented in this work are being revealed during the ongoing observations (e.g. [7, 8]).

Non-thermal synchrotron emission is the main process for radio emission in SNRs (e.g. [9]) produced by highly relativistic particles accelerated at the shock front caused by the expanding shell, as postulated by diffusive shock acceleration theory (e.g. [10]).

In recent years, SNRs at high Galactic latitudes have received some attention, as more objects are detected off the Galactic plane at radio wavelengths. Amongst others, G17.8+16.7 [11], and Ancora SNR (G288.8–6.3; [7, 12]) were detected at high latitudes in γ -rays as well. These SNRs expand in low-density environments with low background noise and diminished risk of source confusion for γ -ray observations. The environment also makes it easier to detect faint diffuse emission in radio and other wavelengths like X-rays.

G310.7–5.4 was first observed and suggested as an SNR candidate by [13]. Our analysis confirms the candidate as an SNR at high Galactic latitude, using EMU/POSSUM survey data from ASKAP. We analysed all relevant available data of the region, including radio intensity, polarisation, and gamma-ray emission.

2. Observations and data processing

2.1 ASKAP

We make use of ASKAP observations [6] from EMU¹ [5] and *Polarisation Sky Survey of the Universe's Magnetism* (POSSUM²; [14]). ASKAP, a radio interferometer consisting of 36 twelve-metre dishes, is located in Western Australia. It has a very wide field of view of approximately 30 deg², making it well-suited for use in surveys.

Stokes I images are taken from the EMU survey, observed at a central frequency of 943.5 MHz with a bandwidth of 288 MHz. Sky maps are convolved to a common angular resolution of 15''. The standard ASKAPsoft [15] pipeline is used for processing observations.

In total, four fields from the EMU/POSSUM survey were used, which were observed between Nov 24, 2022 and Dec 25, 2024. The fields were mosaicked together using corresponding weight files.

¹ASKAP Data Products for Project AS201 (EMU)

²ASKAP Data Products for Project AS203 (POSSUM)

2.2 *Fermi*–LAT

Data from the *Large Area Telescope* (LAT; [17]) aboard the *Fermi* observatory, was used for the γ -ray analysis and a total of 16.5 yr of *Fermi*–LAT Pass 8 data from August 2008 to February 2025 were analysed. A radius of 20° in the region of interest (ROI) centred on the radio SNR at Galactic position $l, b = 310.7^\circ, -5.4^\circ$ was selected in the energy range of 100 MeV to 1 TeV, using a joint, four-component approach adapted from [18]. The latest version of *fermipy* (version 1.2.2; [19]) and *fermitools* v2.2³ software packages were used to analyse the data, together with the latest instrument response function P8R3_SOURCE_V3 and latest *Fermi* catalogue 4FGL–DR4 (v35; [20]).

Sources up to 5° outside the region of interest (ROI) were modelled, and sources up to 20° from the ROI were included in the analysis. Galactic diffuse and isotropic diffuse emission were accounted for using standard methods. Normalisation parameters of sources within 3° , and spectral parameters within 2° , were left to vary during fitting, as were the normalisation factors of sources above a test statistic $TS = 10$ within the ROI. All other source parameters were fixed to their 4FGL–DR4 catalogue values. Fitting was performed using the *newminuit* optimiser.

As the 4FGL–DR4 catalogue shows a source spatially coinciding with G310.7–5.4, we focused on analysing the catalogue source, 4FGL J1413.9–6705, subsequently referred to as J1413. Within 1.0° of G310.7–5.4, three separate 4FGL–DR4 catalogue sources can be found: 4FGL J1413.9–6705 (0.18° angular separation, overlapping with the south-eastern part of the radio shell), 4FGL J1412.1–6631 (0.52°) and 4FGL J1420.7–6701 (0.84°). All other sources are more than 1.4° from the centre of G310.7–5.4. In the analysis, the source position of J1413 was optimised by applying the *localize()* method at energies above 1 GeV.

2.3 Other energy bands

Data from the Wide-field Infrared Survey Explorer (WISE) were used to inspect any hints of a thermal counterpart from the ROI, and strengthen the idea of non-thermal emission from the remnant. Publicly available X-ray data showed no excess emission. Thermal dust maps did also not reveal any significant structured emission.

3. Results

3.1 Radio continuum

A total intensity map from ASKAP at 943.5 MHz of the SNR is presented in Fig. 1. We observe an extended, bilateral, low-surface brightness object, with thin shell-like emissions seen brightest in the western (right) part, as well as the north-eastern (top left) part of the object

The full diameter of G310.7–5.4 is around $30.6'$. Due to the low surface brightness, faint point-like sources, as well as a varying background and missing short spacings resulting in missing flux density for extended diffuse emission, it is quite challenging to measure a reliable flux density. To resolve these challenges, we used methods described in [16], utilising the *polygon_flux* software developed by [21] and determined a flux density of 1.51 ± 0.08 Jy for G310.7–5.4. Uncertainties take into account statistical origins, as well as some systematic effects such as user-based region selection.

³fermi.gsfc.nasa.gov/ssc/data/analysis/documentation/

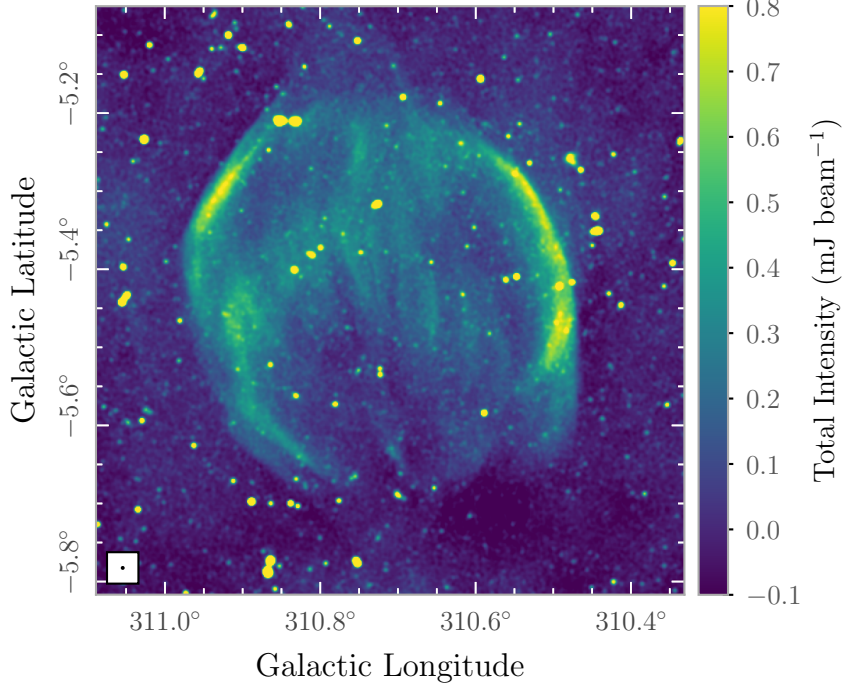


Figure 1: ASKAP 943.5 MHz total intensity image of G310.7–5.4. The synthesised beam of the image is $18'' \times 18''$, represented with a small black circle in the bottom-left corner

3.2 Polarised emission

Polarised intensity (PI) maps show polarised emission throughout different regions of the shell up to $0.3 \text{ mJy beam}^{-1}$. Using the same methods described in the pervious section, we obtain a polarisation flux density of $0.14 \pm 0.03 \text{ Jy}$, resulting in a fractional polarisation of the source of around 9.3 %. The peak polarisation lies around 35 %.

3.3 Infrared results

No spatially correlated IR emission is observed in WISE that may be overlapping with the SNR shell, strongly supporting the evidence for non-thermal emission. For thermal emission, strong correlation at $22 \mu\text{m}$ and $12 \mu\text{m}$ wavelengths would be expected.

3.4 Gamma-ray results

J1413 was modelled with a point-source spatial model and an log-parabola spectral model as taken from the catalogue. Fig. 2 shows the significance map from the γ -ray analysis. While the other *Fermi*–LAT catalogue sources are modelled, the emission attributed to J1413 is shown in the colourmap, and emphasised with significance contours at 2, 3 and 3.5σ levels. Source position optimisation placed J1413 at Galactic position $l, b = 310.75^\circ, -5.55^\circ$ (shown in by the magenta cross and circle). Other *Fermi* sources in the vicinity included 4FGL J1420.7–6701 and

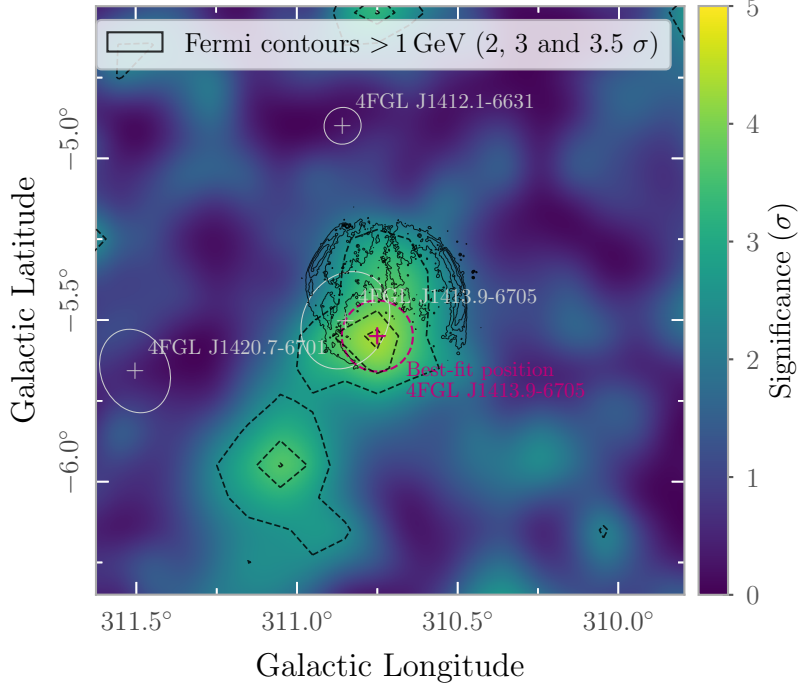


Figure 2: The significance map of the G310.7–5.4 region as seen with *Fermi*–LAT. The optimised position of J1413 is indicated with a magenta cross and circle indicating the best-fit position, and its positional uncertainty. The white markings indicate other respective 4FGL–DR4 sources in the field of view. Thin black contours show radio excess.

4FGL J1412.1–6631, were also modelled. The analysis indicated significant emission coincident with the SNR with a significance of 5.7σ .

4. Discussion and Conclusions

The discovered radio source G310.7–5.4 shows typical radio morphology as seen in other bilateral shell SNRs, such as G296.5+10.0 and SN 1006. The total intensity map (Fig. 1) shows hints of a double shell, which could be explained by a density gradient around the remnant, with one side expanding into a denser medium than the other. There are strong indications that the emission is non-thermal: IR maps from WISE show no correlation between the SNR’s bilateral shell. The source is highly linearly polarised, as expected from synchrotron emission, further supporting the non-thermal origin of the object.

No evidence of non-thermal X-ray emission was found in public data. However, we found a high-energy γ -ray source spatially coinciding with G310.7–5.4 that could be connected to the remnant. With the measured energy flux, it is not possible to determine whether the γ -rays are of leptonic or hadronic origin. However, all confirmed hadronic γ -ray emissions have been seen

in the Galactic plane where SNRs interacted with molecular clouds to accelerate protons that then produce γ -rays via the decay of neutral pions.

G310.7–5.4 is one of a few SNRs that have been discovered displaying γ -ray emission at high Galactic latitudes. In [12], we compiled a list of such sources together with their spatial and spectral γ -ray properties. In addition to detecting another such source, [22] suggested a few more SNRs fitting this subset. An updated compilation of such high Galactic latitude SNRs with γ -ray counterparts can be found in [1].

G310.7–5.4 is now the 13th object of a subset of SNRs off the Galactic plane showing significant high-energy emission [1]. Sources like G310.7–5.4 can be used to study CR escape from SNRs and how they contribute to the Galactic CR population, especially those evolving at high Galactic latitudes, where the risk of source confusion is less pronounced and interactions with clouds are low, allowing the study of the shock properties in unperturbed environments.

For G310.7–5.4, additional radio flux points would allow for spectral index estimation, which instruments like *MeerKAT* could potentially provide. The upcoming *Square Kilometre Array Observatory* (SKAO) will, in its fully operational state, have the ability to detect low-surface brightness objects, such as this source. The upcoming *Cherenkov Telescope Array Observatory* (CTAO) could provide the sensitivity and resolution needed to detect this remnant at very high energies above some tens of GeV. It could also be possible to detect G310.7–5.4 with deep optical observations.

References

- [1] Burger-Scheidlin, C. et al., submitted.
- [2] Green, D. A. 2025, *Journal of Astrophysics and Astronomy* **46** 14
- [3] Acero, F., Ackermann, M., Ajello, M., et al. 2016, *ApJS* **224** 8
- [4] H.E.S.S. Collaboration, et al. 2018, *A&A* **612** A3
- [5] Hopkins, A. M., Kapinska, A., Marvil, J., et al. 2025, *PASA* **42** e071
- [6] Hotan, A. W., Bunton, J. D., Chippendale, A. P., et al. 2021, *PASA* **38** e009
- [7] Filipović, M. D., Dai, S., Arbutina, B., et al. 2023, *AJ* **166** 149
- [8] Ball, B. D., Kothes, R., Rosolowsky, E., et al. 2025, *ApJ* **988** 75
- [9] Berezhko, E. G. & Völk, H. J. 2004, *A&A* **427** 525
- [10] Bell, A. R. 1978, *MNRAS* **182** 147
- [11] Araya, M. 2023, *MNRAS* **518** 4132
- [12] Burger-Scheidlin, C., Brose, R., Mackey, J., et al. 2024, *A&A* **684** A150
- [13] Green, A. J., Reeves, S. N., & Murphy, T. 2014, *PASA* **31** e042

- [14] Gaensler, B. M., Landecker, T. L., Taylor, A. R. & POSSUM Collaboration 2010, in American Astronomical Society Meeting Abstracts, Vol. **215**, American Astronomical Society Meeting Abstracts #215, 470.13
- [15] Guzman, J., Whiting, M., Voronkov, M., et al. 2019, ASKAPsoft: ASKAP science data processor software, Astrophysics Source Code Library, record ascl:1912.003
- [16] Ball, B. D., Kothes, R., Rosolowsky, E., et al. 2023, MNRAS **524** 1396
- [17] Atwood, W. B., Abdo, A. A., Ackermann, M., et al. 2009, ApJ **697** 1071
- [18] Abdollahi, S., Acero, F., Ackermann, M., et al. 2020, ApJS **247** 33
- [19] Wood, M., Caputo, R., Charles, E., et al. 2017, Vol. **301**, 35th International Cosmic Ray Conference (ICRC2017), 824
- [20] Ballet, J., Bruel, P., Burnett, T. H., Lott, B., & collaboration, T. F.-L. 2024, Fermi–Large Area Telescope Fourth Source Catalog Data Release 4 (4FGL-DR4)
- [21] Hurley-Walker, N., Gaensler, B. M., Leahy, D. A., et al. 2019, PASA **36** e048
- [22] Araya, M. 2024, A&A **691** A225